Chemical Engineering Journal 160 (2010) 423–431

Contents lists available at ScienceDirect

Chemical Engineering Journal

journal homepage: www.elsevier.com/locate/cej

CFD modeling of droplet dispersion in a Venturi scrubber

F. Ahmadvand, M.R. Talaie*

Chemical Engineering Department, University of Isfahan, Azadi Sq., University Ave., Isfahan, Iran

ARTICLE INFO

Article history:
Received 3 November 2009
Received in revised form 9 March 2010
Accepted 16 March 2010

Keywords:
Venturi scrubber
CFD modeling
Droplet dispersion
Eddy diffusivity
Droplet size distribution

ABSTRACT

A modified two-dimensional mathematical model was developed to simulate droplet dispersion through a cylindrical Venturi scrubber based on Eulerian approach. Droplet concentration distribution was evaluated using the equation of mass balance of droplets. The velocity field of gas flow was determined using k–ε turbulence model. Droplet velocity distribution was calculated by means of the equations derived using momentum balance of droplets. Gas eddy diffusivity which has already been determined based on constant Peclet number in the previous models was calculated using turbulent characteristic velocity and length. Fathikalajahi et al. approach was applied to calculate eddy diffusivity of droplets (Fathikalajahi et al., 1995 [7]). The mean diameter of generated droplets was determined by Boll's correlation (Boll et al., 1974 [16]). Rosin–Rammler distribution function was used to take into account the distribution of droplet size.

In order to verify the results of the new model a set of experiments was performed on a pilot-scale cylindrical Venturi scrubber with axial liquid injection. During these experiments, the flow rates of liquid droplets were measured at several points of throat section end from center line to the wall. The comparison between the results and experimental data showed that the droplet concentration distribution predicted using the present model were in better agreement with experimental data than that predicted using the previous models which were based on constant Peclet number. Also it was concluded the distribution parameter of Rosin–Rammler function, n_{RR}, could not be considered as a constant parameter and it depended on the L/G (gas to liquid flow rate ratio) and V_{g0} (gas throat velocity).

1. Introduction

In recent years due to growing air pollution problems which are an inevitable result of industry development numerous efforts have been made to develop new air pollution control technologies and to improve the old ones. Venturi scrubbers are one of the most prominent wet scrubbers due to their simple structure, easy application and high removal efficiency. This kind of scrubber utilizes an appropriate liquid (commonly water) to capture particulate and gaseous pollutants from a gas stream. Liquid jet is injected into high speed polluted gas flow which is accelerated using a Venturi-type channel. As a result, injected liquid jet is atomized and a mass of small droplets with different sizes are formed. They disperse in gas due to gas flow and turbulent mixing effect.

The degree of droplet dispersion crucially influences scrubber performance. This is the reason why many theoretical and experimental studies have been performed about droplet dispersion in Venturi scrubbers. A good spatial dispersion of droplets leads to more uniform droplet concentration distribution and hence can increase the scrubber performance. Thus the accurate prediction of droplet dispersion which is controlled by design parameters has critical importance in improving performance and decreasing operating costs of Venturi scrubbers.

While primary models [1,2] had supposed uniform dispersion of droplets in Venturi scrubbers Taheri and Haines [3] performed a pioneering experiment to show the non-uniform dispersion of droplets. Taheri and Sheih [4] have applied a two-dimensional dispersion model to predict droplet concentration distribution assuming that droplets were generated with the same size in a line source for each injected liquid jet. In their model Peclet number was taken equal to 10 and the transversal droplet velocity was ignored. Viswanathan [5] have implemented the following improvements in the previous dispersion model:

1. A point source of droplet generation was used for each injected liquid jet. The location of each point source was predicted by correlation developed to evaluate liquid jet penetration length [6].
2. The initial transversal velocity of droplets was taken equal to transversal component of jet velocity at injection nozzle point.
3. The size distribution was taken into account in the generated droplets.

* Corresponding author. Tel.: +98 031 7934011; fax: +98 03116682887.
E-mail addresses: mrtalaie@eng.ui.ac.ir, mrtalaiekh@yahoo.com (M.R. Talaie).

1385-8947/$ – see front matter © 2010 Elsevier B.V. All rights reserved.
doi:10.1016/j.cej.2010.03.030

Nomenclature

C_d	droplet concentration (No./m^3)
C_D	drag coefficient
D_d	droplet diameter (m)
D_J	jet diameter (m)
D_{32}	Sauter mean diameter (m)
E_d	eddy diffusivity coefficient of droplet (m^2/s)
E_g	eddy diffusivity coefficient of gas (m^2/s)
E	constant in Eq. (3)
f_p	forcing parameter, Eq. (5)
g	gravity acceleration (m/s^2)
l_d	droplet Prandtl mixing length (m)
l_g	gas Prandtl mixing length (m)
L/G	liquid to gas flow rate (m)
$\dot{m}$	droplet generation rate per unit volume (kg/(m s))
n_{RR}	Rosin–Rammler parameter
N_d	number of droplet size segments
N_s	number of droplet source points
Pe	Peclet number $(D\,E_g)/u_g$
Q	total liquid flow rate (m^3/s)
Q_d	local liquid flow rate (m^3/s)
Re	droplet Reynolds number
r	radial coordinate (m)
S_d	droplet generation rate per unit volume (No./(m^3 s))
s	distance traveled by liquid jet from injection point (m)
u	gas velocity in z direction (m/s)
u_d	droplet velocity in z direction (m/s)
$\vec{u}$	gas velocity vector (m/s)
$\vec{u}_d$	droplet velocity vector (m/s)
u'	fluctuation velocity of gas (m/s)
V_g	radial mean gas velocity (m/s)
V_{g0}	gas velocity in throat section (m/s)
V_J	liquid jet velocity (m/s)
v	gas velocity in r direction (m/s)
v_d	droplet velocity in r direction (m/s)
z	axial coordinate (m)

Greek letters

σ	surface tension (kg/s^2)
ρ_g	gas density (kg/m^3)
ρ_l	liquid density (kg/m^3)
μ_l	liquid viscosity (kg/(m s))
ε	turbulence dissipation rate (J/(kg s))
φ	fraction of total mass contained in droplets of diameter less than D_d
β	constant in Eq. (5)
λ	wavelength (m)
ν_{t_g}	gas turbulent dynamic viscosity (m^2/s)
ν_g	gas molecular dynamic viscosity (m^2/s)
υ	viscous damping parameter, Eq. (7) (m^2/s)
χ	characteristic parameter in the Rosin–Rammler function (m)

Subscripts

0	throat section
d	droplet
g	gas
J	liquid jet
l	liquid
i	refers to droplet source location
j	refers to droplet diameter

Table 1
The values of the parameters used in Adelberg's equation [8].

Parameter	Value
β	0.348
K_A	1
e	0.4
K_P	0.1145

Fathikalajahi et al. [7] have improved this model by means of introducing a way to evaluate droplet eddy diffusivity coefficient. They have specified an eddy as a single entity passing a distance during its residence time that was calculated with Prandtl Mixing Length Theory. Gonçalves et al. [8] have enhanced the previous models by predicting the trajectory of liquid jet which was atomized continuously until it disappeared. They have considered the liquid jet path as the locations of point sources for droplet generation [9]. Pak and Chang [10] developed an Eulerian–Lagrangian computational model for the interactive three-phase flow in a Venturi scrubber in order to estimate pressure drop and collection efficiency. The KIVA code was used to simulate this three-phase flow model which included interaction between gas and droplets atomization of a liquid jet, droplet deformation, break-up and collision of droplets, and capture of dust by droplets. Because of using software to simulate droplet dispersion and particle collection in a Venturi scrubber the details of the used approaches to find the important parameters such as droplet eddy diffusivity, liquid jet modeling, . . . were not reported in this work. Talaie et al. [11] have performed a theoretical and experimental study to show that Peclet number could not be constant across the cross section of Venturi scrubber. They have concluded that for better prediction of droplet concentration distribution, the radial variation of Peclet number must be taken into account.

The main objective of the present work was to study droplet dispersion in Venturi scrubbers both experimentally and theoretically. A modified mathematical model was introduced which differed from the earlier works of Fathikalajahi et al. [7], Gonçalves et al. [8] and Talaie et al. [11] in applying two-dimensional velocity profile for gas and droplets based on Eulerian approach and computing gas eddy diffusivity using k–ε turbulence model. While in the previous models a constant Peclet number was used to find gas eddy diffusivity. The accuracy of the developed model was tested by comparing its results with the experimental data obtained in this study for a cylindrical pilot-scale Venturi scrubber.

2. Mathematical model

2.1. The assumptions made in the model

1. The Venturi scrubber is cylindrical type.
2. The liquid jet was injected axially through a single nozzle into the gas flow at the center of the Venturi channel.
3. Gas velocity field and droplet concentration distribution were symmetrical around the center line of the Venturi scrubber.
4. The gas flow field was determined by solving Reynolds and continuity equations and employing k–ε turbulence model. It was also

Table 2
The information of the carried out experiments.

Liquid flow rate (l/min)	Gas throat velocity		
	60 m/s	75 m/s	85 m/s
1.0	–	√	–
2.0	√	√	√
4.0	√	√	√

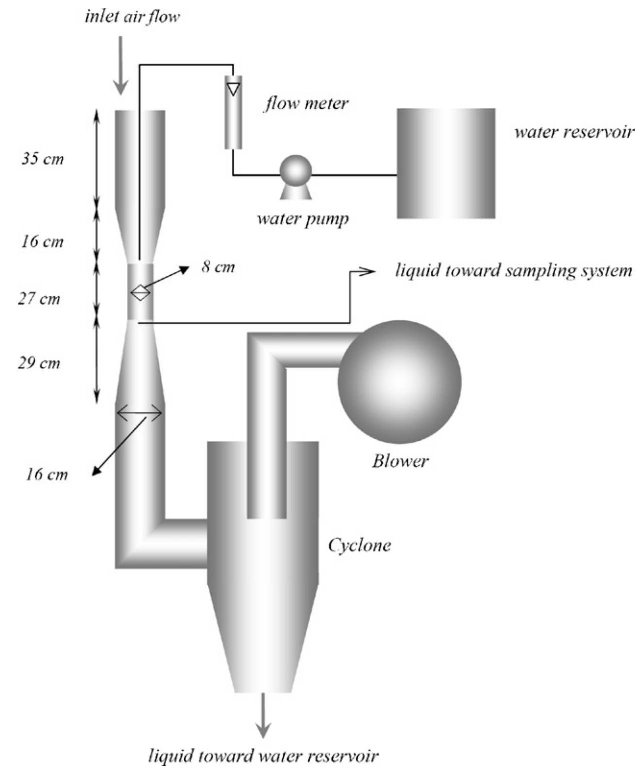

Fig. 1. The schematic diagram of experimental set-up.

assumed that the flow field was not influenced by the presence of droplets.

5. Only gas turbulence was responsible for radial dispersion of droplets.
6. The droplets were generated along the liquid jet path as a result of jet break-up. Thus liquid jet path was divided into several segments each to be considered as a point source for droplet parcels. Each parcel contained a certain number of droplets with identical characteristics (their sizes, source locations and hence initial velocities).

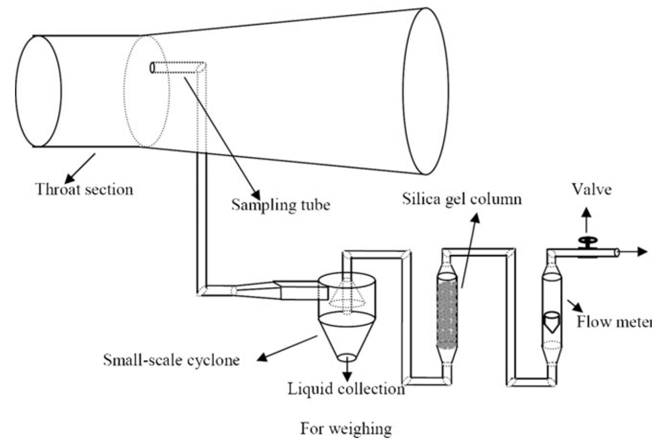

Fig. 2. The sketch of sampling system.

According to assumption 6, droplet parcels could be classified based on their source locations and diameters. Therefore, the characteristics of droplets belonging to different parcels were distinguished by two subscripts i and j standing for their source location and size, respectively.

2.2. Governing equations

The following continuity equation was used to determine droplet concentration distribution in Venturi channel:

$$\frac{\partial}{\partial z}\left(rC_{dij}u_{dij} - rE_{dj}\frac{\partial C_{dij}}{\partial z}\right) + \frac{\partial}{\partial r}\left(rC_{dij}v_{dij} - rE_{dj}\frac{\partial C_{dij}}{\partial r}\right) = rS_{dij} \quad (1)$$

In the above equation C_{dij} is the number concentration of droplets with diameter D_{dj} produced in source point i, u_{dij} and v_{dij} are the z and r components of droplet velocity vector, E_{dj} is droplet eddy diffusivity and S_{dij} refers to the rate of droplet generation per unit of volume which was calculated based on liquid jet trajectory and atomization rate.

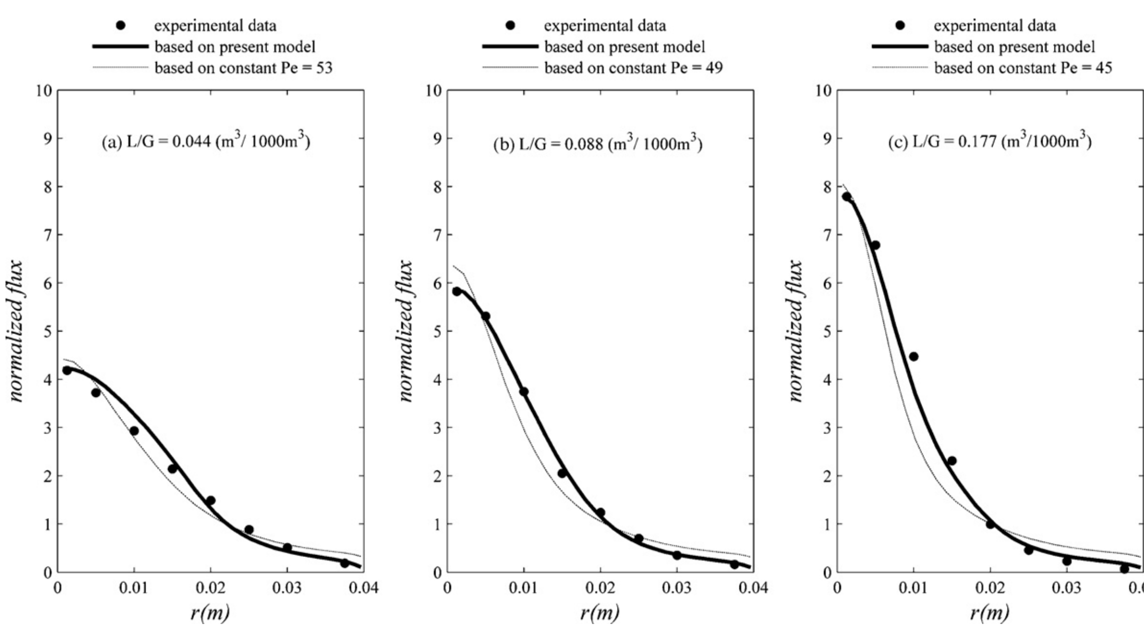

Fig. 3. The radial variation of normalized flux at the end of the throat section; comparison between the results calculated based on the present model and those obtained based on constant Peclet number with the experimental data for V_{g0} equal to 75 m/s and three different values of L/G.

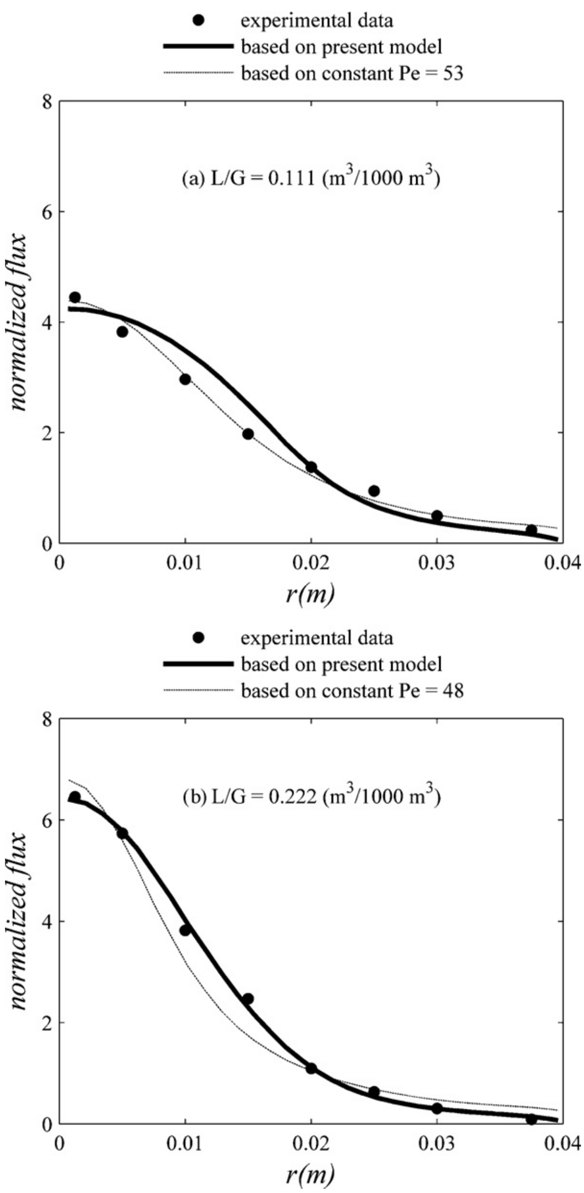

Fig. 4. The radial variation of normalized flux at the end of the throat section; comparison between the results calculated based on present model and those obtained based on constant Peclet number with the experimental data for V_{g0} equal to 60 m/s and three different values of L/G.

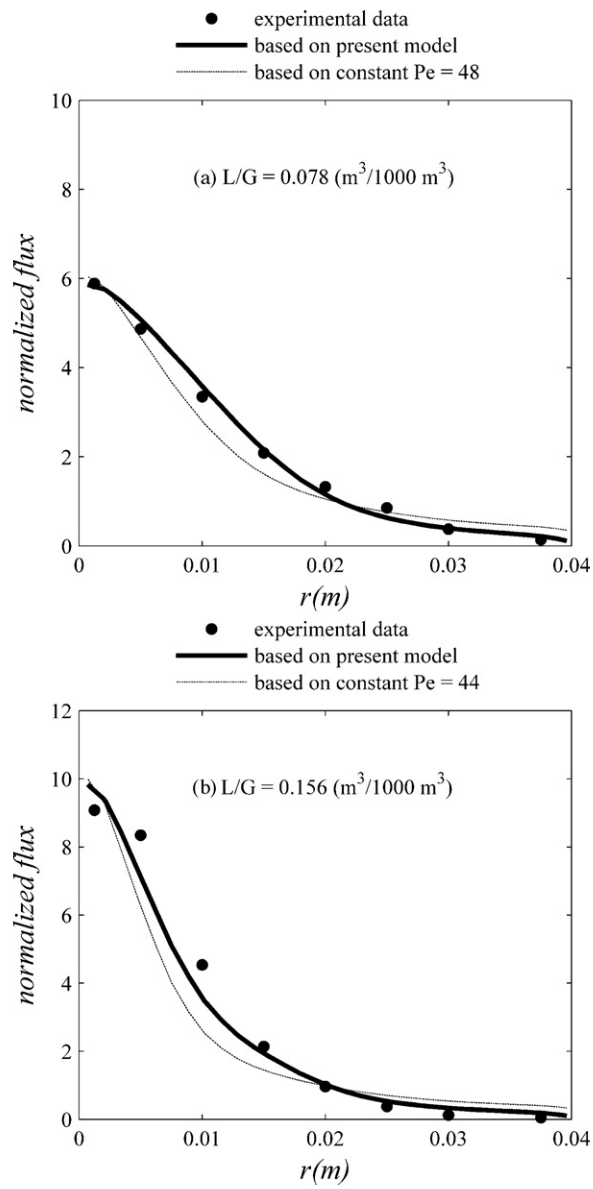

Fig. 5. The radial variation of normalized flux at the end of the throat section; comparison between the results calculated based on present model and those obtained based on constant Peclet number with the experimental data for V_{g0} equal to 85 m/s and three different values of L/G.

The jet trajectory was found by solving mass and momentum conservative differential equations written for liquid jet, as follows:

$$\frac{\pi}{2}\rho_l V_J D_J \frac{dD_J}{ds} + \frac{\pi}{4}\rho_l D_J^2 \frac{dV_J}{ds} + \dot{m} = 0 \quad (2)$$

$$\frac{\pi}{2}\rho_l \left(V_J D_J^2 \frac{dV_J}{ds} + V_J^2 D_J \frac{dD_J}{ds} \right) + \dot{m} V_J + \frac{1}{2} C_{Drag} \pi D_J \rho_g |V_g - V_J|(V_g - V_J) - \frac{\pi}{4}\rho_l D_J^2 g = 0 \quad (3)$$

where D_J and V_J are the diameter and velocity of jet respectively, $\dot{m}$ is the atomization rate of liquid jet and s is the distance passed by the liquid jet (axial distance from the injection point). The rate of atomization of liquid jet was calculated based on the study performed by Adelberg [12]. He has assumed that the formation and growth of the waves were the main mechanism for jet atomization. Based on this assumption the following equation for the rate of atomization per unit length of liquid jet has been introduced:

$$\dot{m} = \frac{K_A \rho_l}{eD_J - \lambda_{m\sigma}} \left\{ \frac{2}{5} f_P [(eD_J)^{5/2} - {\lambda_{m\sigma}}^{5/2}] - \upsilon [eD_J - \lambda_{m\sigma}] \right\} \quad (4)$$

In the above equation f_P is force parameter, υ is viscous damping parameter and $\lambda_{m\sigma}$ is the minimum wavelength. These parameters were determined by the following equations:

$$f_P = \frac{\beta (\pi/2)^{1/2} \rho_g V_g^2}{(\rho_l \sigma)^{1/2}} \quad (5)$$

$$\upsilon = \frac{8\pi^2 \mu_l}{\rho_l} \quad (6)$$

$$\lambda_{m\sigma} = 15.8326 \left[\frac{\mu_l (\sigma/\rho_l)^{1/2}}{\beta \rho_g V_g^2} \right]^{2/3} \quad (7)$$

The values of the parameters used in the present model were according to Table 1. With simultaneous solving Eqs. (2)–(4), diameter and velocity of liquid jet and also the rate of liquid atomization per unit length would be found as a function of s.

Velocity distribution of droplets belonging to each parcel (denoted by ij) was determined by means of the following equations expressing Eulerian droplet momentum balance:

$$\frac{\partial}{\partial z}\left(u_{dij}\left(rC_{dij}u_{dij} - rE_{dj}\frac{\partial C_{dij}}{\partial z}\right)\right) + \frac{\partial}{\partial r}\left(u_{dij}\left(rC_{dij}v_{dij} - rE_{dj}\frac{\partial C_{dij}}{\partial r}\right)\right) = \frac{3}{4}\frac{\rho_g}{\rho_l}\frac{C_D}{D_{dj}}|\vec{u} - \vec{u}_{dij}|(u - u_{dij})rC_{dij} + rC_{dij}g \quad (8)$$

$$\frac{\partial}{\partial z}\left(v_{dij}\left(rC_{dij}u_{dij} - rE_{dj}\frac{\partial C_{dij}}{\partial z}\right)\right) + \frac{\partial}{\partial r}\left(v_{dij}\left(rC_{dij}v_{dij} - rE_{dj}\frac{\partial C_{dij}}{\partial r}\right)\right) = \frac{3}{4}\frac{\rho_g}{\rho_l}\frac{C_D}{D_{dj}}|\vec{u} - \vec{u}_{dij}|(v - v_{dij})rC_{dij} \quad (9)$$

In the above equations $\vec{u}$ and $\vec{u}_{dij}$ are the gas and droplet velocity vectors and C_D is the drag coefficient for droplets.

Marshal–Dickenson relation that is valid for $Re_d < 3000$ [8] was applied for drag coefficient:

$$C_D = 0.22 + \frac{24(1 + 0.15\,Re_d^{0.6})}{Re_d} \quad (10)$$

$$Re_d = \frac{|\vec{u}_g - \vec{u}_d|D_d}{\nu} \quad (11)$$

Droplet eddy diffusivity coefficient was evaluated based on the work of Fathikalajahi et al. [7]. The eddy diffusivity of droplet was correlated to gas eddy diffusivity by the following equation:

$$\frac{E_d}{E_g} = \frac{l_d^2}{l_g^2} \quad (12)$$

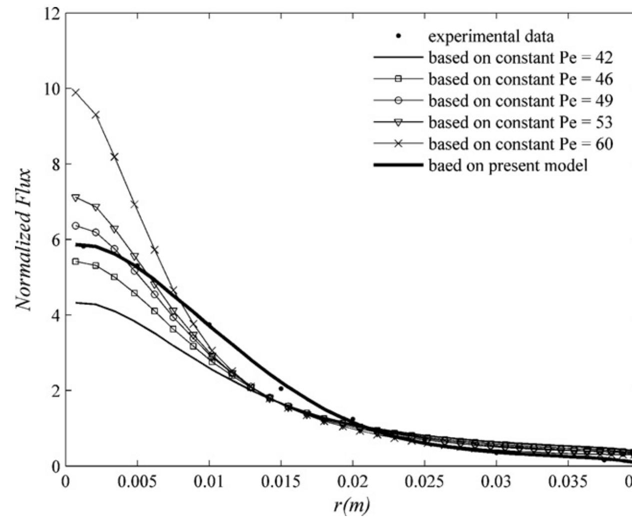

Fig. 6. The radial variation of normalized flux at the end of the throat section; comparison between the results calculated based on present model and those obtained based on various constant Peclet numbers with the experimental data for V_{g0} = 75 m/s and L/G = 0.088 m^3/1000 m^3.

where l_d and l_g are the Prandtl mixing lengths of droplets and gas, respectively. This method and the involved equations were detailed in Ref. [7].

In order to evaluate E_d, the gas eddy diffusivity coefficient should be determined. In all previous studies a constant Peclet number has been utilized for estimating E_g. However in this study E_g was determined by Tenekes–Lumley equation [13]:

$$E_g = c_1 u' l \quad (13)$$

where u' and l are characteristic velocity and length, respectively. The characteristic velocity u' can be considered equal to square root of turbulence kinetic energy, k. The characteristic length, l, can be

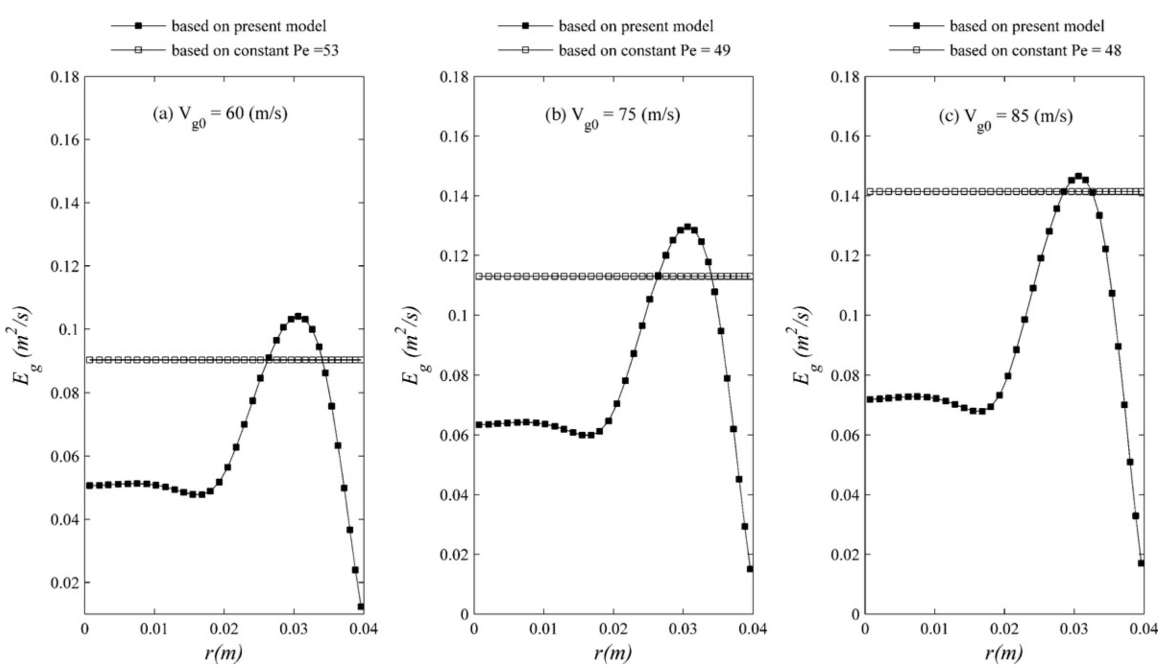

Fig. 7. The radial variation of eddy diffusivity of gas at the end of the throat; comparison between the values of E_g calculated using present model and those obtained using constant Peclet number for different gas throat velocities.

defined in terms of turbulence characteristics [14] as follows:

$$l = \frac{3u'^3}{2\varepsilon} \quad (14)$$

where ε is the rate of dissipation of turbulence kinetic energy. The value of c_1 usually was determined by fitting with experimental data [14].

Rosin–Rammler function was applied for considering the size distribution of droplets according to Fernandez Alonso et al. study [15]:

$$1 - \varphi = \exp\left(-\left(\frac{D_d}{\chi}\right)^{n_{RR}}\right) \quad (15)$$

where φ is the volume fraction of droplets having diameter smaller than D_d and n_{RR} is the parameter which can change the size distribution width. Decreasing n_{RR} reduces the spread of size distribution. The parameter χ is correlated to the Sauter mean diameter, D_{32}, using the following equation:

$$\frac{\chi}{D_{32}} = \Gamma\left(1 - \frac{1}{n_{RR}}\right) \quad (16)$$

Fernandez Alonso et al. [15] have suggested the constant value of 2.15 for n_{RR}. Also they concluded that Boll's equation [16] could be applied for accurate calculation of Sauter mean diameter. The SI unit form of this equation is as follows:

$$D_{32} = \frac{4.22 \times 10^{-2} + 5.77 \times 10^{-3}(1000L/G)^{1.922}}{V_{g0}^{1.602}} \quad (17)$$

The total local concentration of droplets was obtained with the following summation:

$$C_d = \sum_i^{N_s}\sum_j^{N_d} C_{dij} \quad (18)$$

where N_s and N_d are the number of droplet source points and diameter groups, respectively. Also the total local flow rate of droplets was calculated by similar summation as follows:

$$Q_d = \sum_i^{N_s}\sum_j^{N_d}\left(\frac{\pi}{6}D_{dj}^3\rho_l C_{dij}\right) \quad (19)$$

The gas velocity components, u and v, turbulence kinetic energy, k, and the rate of dissipation of turbulence kinetic energy, ε, were obtained by solving Reynolds and continuity equations and the relations related to standard k–ε turbulence model. These equations are given as follows:

continuity equation

$$\frac{\partial(rv)}{\partial r} + \frac{\partial(ru)}{\partial z} = 0 \quad (20)$$

Reynolds equation in z direction

$$\frac{\partial}{\partial r}\left(ruv - r(\nu_{t_g} + \nu_g)\frac{\partial u}{\partial r}\right) + \frac{\partial}{\partial z}\left(ru^2 - r(2\nu_{t_g} + \nu_g)\frac{\partial u}{\partial z}\right) = -\frac{r}{\rho_g}\frac{\partial p}{\partial z} + \frac{\partial}{\partial}\left(r\nu_{t_g}\frac{\partial v}{\partial z}\right) \quad (21)$$

Reynolds equation in r direction

$$\frac{\partial}{\partial r}\left(rv^2 - r(2\nu_{t_g} + \nu_g)\frac{\partial v}{\partial r}\right) + \frac{\partial}{\partial z}\left(ruv - r(\nu_{t_g} + \nu_g)\frac{\partial v}{\partial z}\right) = -\frac{r}{\rho_g}\frac{\partial p}{\partial r} - (2\nu_{t_g} + \nu_g)\frac{v}{r} + \frac{\partial}{\partial z}\left(r\nu_{t_g}\frac{\partial u}{\partial r}\right) \quad (22)$$

Turbulent kinetic energy, k, equation

$$\frac{\partial}{\partial r}\left(rvk - r\left(\frac{\nu_{tg}}{\sigma_k} + \nu_g\right)\frac{\partial k}{\partial r}\right) + \frac{\partial}{\partial z}\left(ruk - r\left(\frac{\nu_{tg}}{\sigma_k} + \nu_g\right)\frac{\partial k}{\partial z}\right) = -r\varepsilon + r\nu_{t_g}G \quad (23)$$

Dissipation rate of turbulent kinetic energy, ε, equation

$$\frac{\partial}{\partial r}\left(rv\varepsilon - r\left(\frac{\nu_{tg}}{\sigma_\varepsilon} + \nu_g\right)\frac{\partial \varepsilon}{\partial r}\right) + \frac{\partial}{\partial z}\left(ru\varepsilon - r\left(\frac{\nu_{tg}}{\sigma_\varepsilon} + \nu_g\right)\frac{\partial \varepsilon}{\partial z}\right) = -C_1\nu_{t_g}Gr\frac{\varepsilon}{k} + C_2 r\frac{\varepsilon^2}{k} \quad (24)$$

In the above equations ν_{tg} is turbulent viscosity and G is the generation of turbulent kinetic energy. The parameters G and ν_{tg} were calculated using the following relations:

$$G = \left[2\left(\frac{\partial v}{\partial r}\right)^2 + 2\frac{v^2}{r^2} + 2\left(\frac{\partial u}{\partial z}\right)^2 + \left(\frac{\partial u}{\partial z} + \frac{\partial v}{\partial r}\right)^2\right] \quad (25)$$

$$\nu_{t_g} = \rho_g C_\mu \frac{k^2}{\varepsilon} \quad (26)$$

2.3. Method of solution

Numerical solution of governing equations was performed by the finite volume method. SIMPLE algorithm was used to solve Eqs. (20)–(26). Also Power-law scheme along with staggered grid system [17] was employed to obtain numerical solution of Eqs. (1), (8) and (9).

2.4. Boundary conditions

Due to symmetric assumption the radial gradients of C_d, u_d and v_d were assumed to be zero at the center line:

$$\left(\frac{\partial C_d}{\partial r}\right)_{center\ line} = \left(\frac{\partial u_d}{\partial r}\right)_{center\ line} = \left(\frac{\partial v_d}{\partial r}\right)_{center\ line} = 0 \quad (27)$$

Also it was assumed that droplet flux across the wall was zero:

$$\left(\frac{\partial C_d}{\partial r}\right)_{wall} = 0 \quad (28)$$

$$(u_d)_{wall} = (v_d)_{wall} = 0 \quad (29)$$

The common boundary conditions were used for k–ε turbulence model. They can be found in many published works in literature [18].

3. Experiment

The experimental set-up is shown in Fig. 1. The cylindrical Venturi scrubber which was the main part of this set-up was assembled vertically. The diameter of throat was 8 cm and the diameters of the inlets of both converging and diverging sections were 16 cm. The other dimensions of the Venturi scrubber are displayed in this figure. Liquid was injected through a single nozzle with diameter of 7 mm at the center of the throat entrance concurrently with gas stream. The flow rates of droplets were measured at several points of the end of throat section by using sampling system shown in Fig. 2. The sampling tube had an inner diameter of 5 mm. The gas flow rate through sampling system was adjusted so that the iso-kinetic sampling condition was satisfied (the gas velocity at the entrance of sampler tube was equal to the gas velocity). The experiments were carried out according to the characteristics given in Table 2.

4. Results and discussion

In this section the developed model was verified by comparing the calculated and experimentally obtained liquid flux distributions. Also these results were compared with those obtained by using a constant Peclet number to estimate E_g. The effect of gas eddy diffusivity, Peclet number and droplet size distribution on droplet dispersion throughout Venturi scrubber was discussed by using the presented model.

4.1. Model verification

In order to show the ability of the new model for better prediction of droplet dispersion, the results of this model were compared with those of the model based on a constant Peclet number. This constant Peclet number was obtained by fitting the results of the model with the experimental data for each condition. Also the results of the new model were obtained by adjusting the values of n_{RR} and c_1 (the parameters of Eqs. (13) and (15)) to attain the best agreement with experimental data. Because c_1 was not dependent on droplet size and liquid flow rate it was considered as a constant fitting parameter. The value of 1.65 was obtained for c_1 by optimization procedure. Also the different values of n_{RR} were obtained for different operational conditions. Figs. 3–5 show the radial variations of normalized flux across the cross sectional area of throat end for three values of 60, 75, 85 m/s for V_{g0} and different values of L/G (these values are displayed on this figure). As can be seen in these figures, the results of the new model are in better agreement with the experimental data. This better agreement can be attributed mainly to the fact that the variation of eddy diffusivity was included in the new model using k–ε turbulent model parameters.

Fig. 6 shows the effect of Peclet number on the calculated droplet concentration distribution using the model based on constant Peclet number. Also these results were compared with the best fitted results of the present model in this figure. All calculated results were obtained for the condition of V_{g0} = 75 m/s and L/G = 0.088 m^3/1000 m^3. As it can be seen in this figure the results of the constant Peclet model cannot coincide with the present model for any used Peclet number. This discrepancy can be attributed to the fact that the Peclet number cannot be considered constant across the cross section on Venturi channel.

Figs. 7 and 8 show the variations of gas and droplets eddy diffusivity across the cross sectional area of the throat end. Because in the new model the effect of the presence of droplets on the turbulence intensity of gas flow was ignored, the values of gas eddy diffusivity was solely related to the gas velocity.

4.2. Peclet number and eddy diffusivity

A spray of droplets laden in a turbulent flow can be dispersed due to turbulent mixing effect. The degree of droplet dispersion depends on droplet diameter, liquid characteristics and the intensity of turbulence [19]. For the case of Venturi scrubber with axial liquid injection, the turbulent diffusion mechanism is solely responsible for transversal droplet dispersion [11]. Thus the accurate prediction of turbulent gas diffusivity is important in simulating droplet dispersion especially for this kind of Venturi scrubber.

Although in all previous models Peclet number was considered to be constant, the appropriate value of this dimensionless number and its dependence on the operating parameters like gas throat velocity and L/G has been under controversy. Through several studies performed in mathematical modeling of droplet dispersion in a Venturi scrubber, the various values have been reported for Peclet number [4,7,8,20]. In all of these works, gas eddy diffusivity has been calculated using constant Peclet number and droplet concentration distribution has been fitted to the experimental data by using Peclet number as the sole fitting parameter. However droplet dispersion is a complex function of factors such as mean droplet diameter, droplet size distribution, the method of liquid injection, the liquid jet trajectory, the rate of liquid jet atomization, gas eddy diffusivity and mean gas velocity. In this way, the effects of these factors on droplet dispersion may be included into the fitted values of Peclet number. This is the reason why different researchers have been reported different values for Peclet number.

Fig. 7 shows the radial variations of the calculated E_g at the end of throat section for throat velocities of 60, 75 and 85 m/s. In this figure the values of E_g obtained based on the fitted constant Peclet number were compared with those calculated based on k–ε turbulence model. As it can be seen gas eddy diffusivity rises appreciably

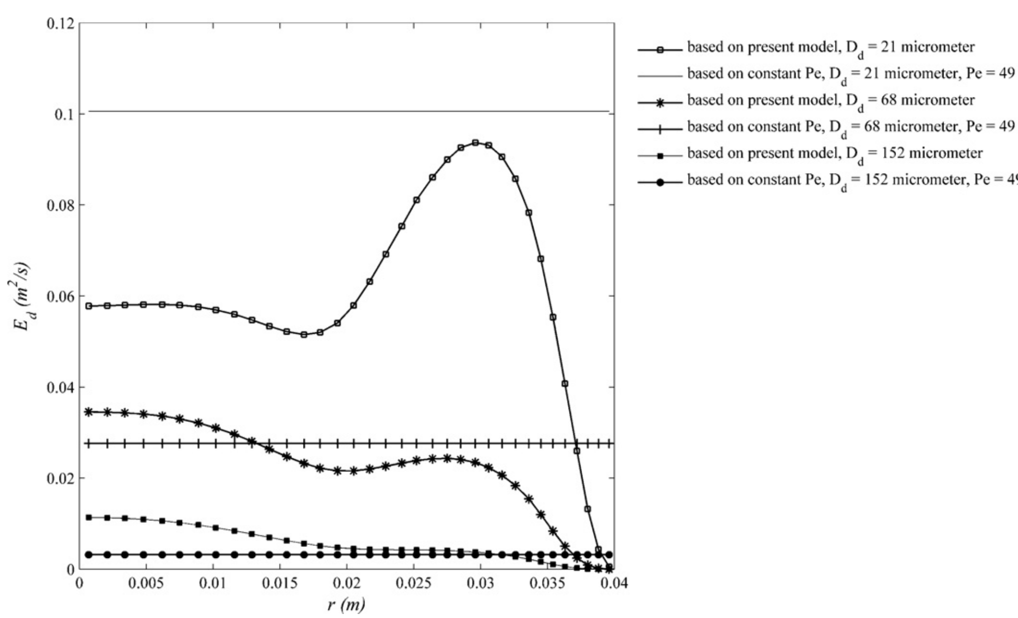

Fig. 8. The radial variation of eddy diffusivity of droplets at the end of the throat; comparison between the values of E_d calculated using the present model and those obtained using constant Peclet number for V_{g0} = 75 m/s and L/G = 0.088 m^3/1000 m^3 and three different droplet diameters.

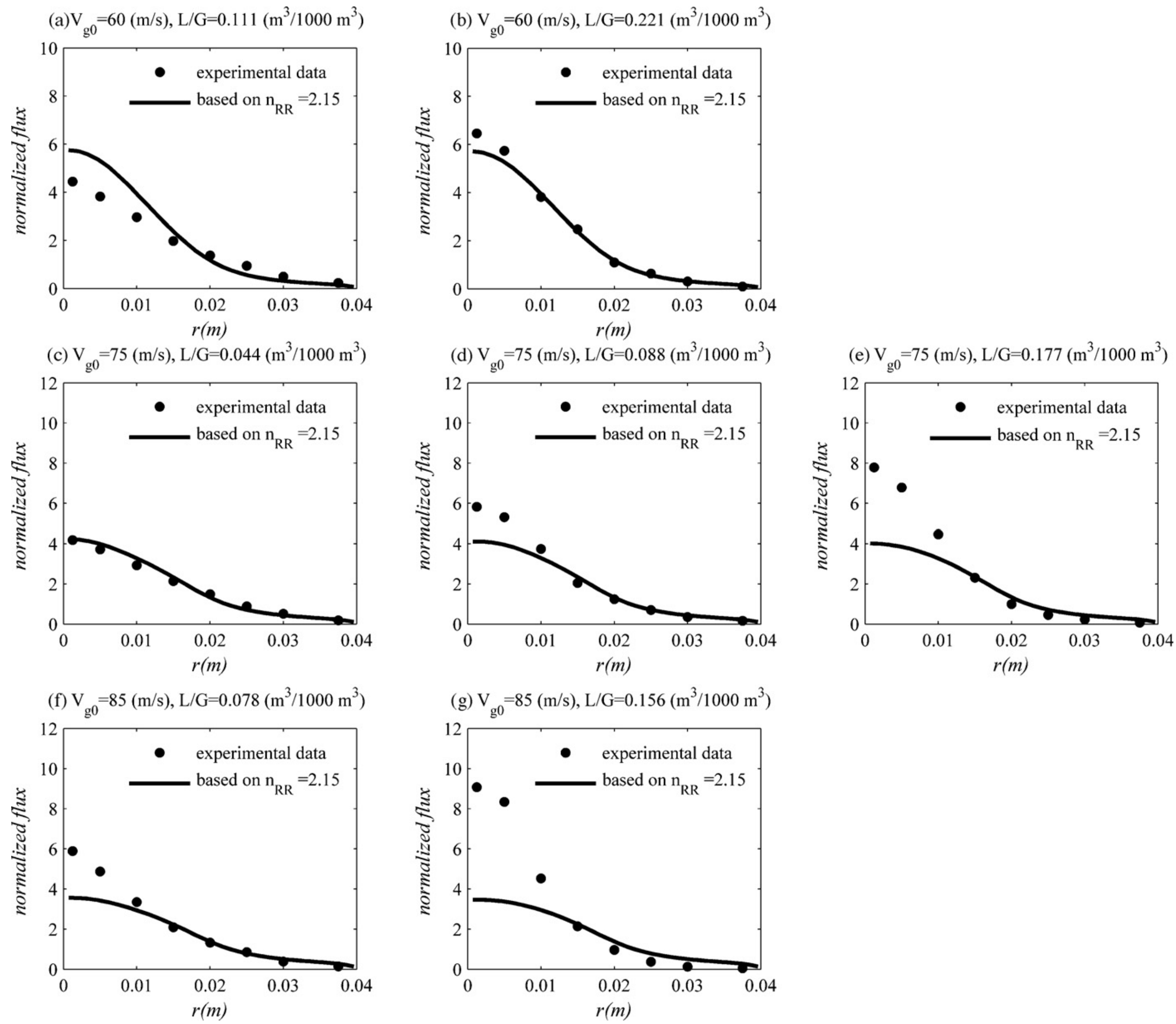

Fig. 9. The radial variation of normalized flux at the end of the throat section; comparison between the best fitted results obtained based on n_{RR} equal to 2.15 with experimental dada for different values of V_{g0} and L/G.

as gas velocity increases. Fig. 8 shows the variation of droplet eddy diffusivity across the cross sectional area of throat end for three droplet diameters of 21, 68 and 159 μm at gas throat velocity of 75 m/s. Also the droplet eddy diffusivity calculated based on the fitted constant Peclet number was presented in this figure for the same conditions. As it can be seen increasing droplet size decreases the droplet eddy diffusivity.

4.3. Droplet size distribution

As mentioned, droplet size influences droplet eddy diffusivity and hence affects on the degree of droplet dispersion. Droplets, whose sizes are small enough, follow turbulent eddy motion. However larger droplets have eddy diffusivity less than gas [4,19]. Thus the size distribution wide of formed droplets can affect on droplet concentration distribution significantly. Some experimental and theoretical studies have shown that the exponent n_{RR} in Rosin–Rammler function can be adjusted to make agreement between theoretical and experimental results. This explains why the different values have been reported for n_{RR} (between 1.6 and 2.7) which were obtained in different operational conditions [11,15,21].

In order to investigate the influence of the operational conditions like V_{g0} and L/G on parameter n_{RR} the model was fitted on the experimental data by adjusting the value of c_1 and using a constant value of 2.15 for n_{RR}. This value was obtained equal 1.7 by the optimization procedure. The results of this fitted model were compared with the experimental data at Fig. 9. As it appears, the model is not capable of predicting experimental data well. This fact reveals that parameter n_{RR} cannot be considered as a constant and should be a function of V_{g0} and L/G.

5. Conclusion

Upon the results of this study the following conclusions can be drawn:

- Using CFD modeling instead of using one-dimensional gas velocity and constant Peclet number can improve the agreement between the results of the model and experimental data.

- The determination of gas eddy diffusivity and droplet size distribution are two important parts of the comprehensive model which needs special attention.
- Turbulence characteristics k and ε can be used to evaluate the gas eddy diffusivity throughout the Venturi scrubber.
- The distribution parameter of Rosin–Rammler function, n_{RR}, cannot be considered constant. It depends on L/G and V_{g0}. Further investigations need to be carried out for a correlation between this parameter and operating parameters.

References

[1] S. Calvert, Venturi and other atomizing scrubbers' efficiency and pressure drop, AIChE J. 16 (1970) 392–396.
[2] R.H. Boll, Particle collection and pressure drop in Venturi scrubbers, Ind. Eng. Chem. Fundam. 12 (1973) 40–50.
[3] M. Taheri, G.F. Haines, Optimization of factors affecting scrubber performance, J. Air Pollut. Control Assoc. 19 (1969) 427–431.
[4] M. Taheri, Ch.M. Sheih, Mathematical modeling of atomizing scrubbers, AIChE J. 16 (1) (1975) 153–157.
[5] Sh. Viswanathan, Modeling of Venturi scrubber performance, Ind. Eng. Chem. Res. 36 (1997) 4308–4317.
[6] Sh. Viswanathan, C.C. St Pierre, A.W. Gnyp, Jet penetration measurements in a Venturi scrubber, Can. J. Chem. Eng. 61 (1983) 504–508.
[7] J. Fathikalajahi, M.R. Talaie, M. Taheri, Theoretical study of liquid droplet dispersion in a Venturi scrubber, Air Waste Manage. Assoc. 45 (1995) 181–185.
[8] J.A.S. Gonçalves, M.A.M. Costa, M.L. Aguiar, J.R. Coury, Atomization of liquids in a Pease-Anthony Venturi scrubber. Part II: Droplet dispersion, J. Hazard. Mater. B116 (2004) 147–157.
[9] J.A.S. Gonçalves, M.A.M. Costa, P.R. Henrique, J.R. Coury, Atomization of liquids in a Pease-Anthony Venturi scrubber. Part I: Jet dynamic, J. Hazard. Mater. B97 (2003) 267–279.
[10] S.I. Pak, K.S. Chang, Performance estimation of a Venturi scrubber using a computational model for capturing dust particles with liquid spray, J. Hazard. Mater. 138 (B) (2006) 560–573.
[11] M.R. Talaie, N. Mokhtarian, A.R. Talaie, M. Karimikhosroabadi, F. Sadeghi, Experimental and theoretical investigation of droplet dispersion in Venturi scrubbers with axial liquid injection, Chem. Eng. Technol. 32 (5) (2009) 798–804.
[12] M. Adelberg, Breakup rate and penetration of a liquid jet in a gas stream, AIAA J. 5 (1967) 1408–1415.
[13] H. Tenekes, J.L. Lumley, A First Course in Turbulence, MIT Press, Cambridge, 1972.
[14] A. Mohebbi, M. Taheri, J. Fathikalajahi, M.R. Talaie, Simulation of an orifice scrubber performance based on Eulerian/Lagrangian method, J. Hazard. Mater. A100 (2003) 13–25.
[15] D. Fernandez Alonso, J.A.S. Gonçalves, B.J. Azzopardi, Drop size measurements in Venturi scrubbers, Chem. Eng. Sci. 56 (2001) 4901–4911.
[16] R.H. Boll, L.R. Flais, P.W. Maurer, W.L. Thompson, Mean drop size in a full scale Venturi scrubber via transmissometer, J. Air Pollut. Control Assoc. 24 (1974) 934–938.
[17] S.V. Patankar, Numerical Heat Transfer and Fluid Flow, McGraw-Hill, New York, 1980.
[18] H.K. Versteeg, W. Malalasekera, An Introduction to Computational Fluid Dynamics the Finite Volume Method, Prentice Hall, London, 1995.
[19] A. Altunbaş, G. Kelbaliyev, K. Ceylan, Eddy diffusivity of particles in turbulent flow in rough channels, J. Aerosols Sci. 33 (2002) 1075–1086.
[20] S. Viswanathan, A.W. Gnyp, C.C. St. Pierre, Examination of gas flow in a Venturi scrubber, Ind. Eng. Chem. Fundam. 23 (1984) 303–308.
[21] M.A.M. Costa, P.R. Henrique, J.A.S. Gonçalves, J.R. Coury, Droplet size in a rectangular Venturi scrubber, Braz. J. Chem. Eng. 21 (02) (2004) 335–343.